

## A Microfluidic Rectifier: Anisotropic Flow Resistance at Low Reynolds Numbers

Alex Groisman\* and Stephen R. Quake†

Department of Applied Physics, California Institute of Technology, MS 128-95, Pasadena, California 91125, USA

(Received 17 September 2003; published 4 March 2004)

It is one of the basic concepts of Newtonian fluid dynamics that at low Reynolds number ( $Re$ ) the Navier-Stokes equation is linear and flows are reversible. In microfluidic devices, where  $Re$  is essentially always low, this implies that flow resistance in microchannels is isotropic. Here we present a microfluidic rectifier: a microscopic channel of a special shape whose flow resistance is strongly anisotropic, differing by up to a factor of 2 for opposite flow directions. Its nonlinear operation at arbitrary small  $Re$  is due to non-Newtonian elastic properties of the working fluid, which is a 0.01% aqueous solution of a high molecular weight polymer. The rectifier works as a dynamic valve and may find applications in microfluidic pumps and other integrated devices.

DOI: 10.1103/PhysRevLett.92.094501

PACS numbers: 47.50.+d, 83.10.Bb, 47.85.Np

The idea of a fluidic rectifier (a channel whose resistance depends on the direction of flow) was suggested in the early 20th century by Tesla [1]. In 1920 he patented the “valvular conduit,” a channel network consisting of an open main duct and a set of side loop channels joining the duct at sharp angles. The operation of Tesla’s device relies on the inertia of the fluid and is efficient only for high Reynolds number flows. Indeed, when the Reynolds number,  $Re$ , is low the nonlinear inertial term in the Navier-Stokes equation is small, and the equation becomes linear [2]:  $\eta\Delta\vec{V} - \vec{\nabla}P = 0$ . Here  $V$  is velocity,  $P$  is pressure, and  $\eta$  is viscosity of the fluid. Because this equation is invariant under the transformation  $V \rightarrow -V$ ,  $P \rightarrow -P$ , the flow should be completely reversible. Therefore, at low  $Re$  the resistance of a channel should be the same for both flow directions, independent of the channel shape.

The question of whether or not it is possible to construct a low  $Re$  rectifier has important practical applications in the field of microfluidics. The characteristic driving pressure per unit length,  $\Delta P/\Delta L$ , needed to reach a given average flow velocity  $\bar{V}$  in a channel of diameter  $D$ , scales like  $\Delta P/\Delta L \sim \bar{V}/D^2$ . Since  $Re$  can be defined as  $\rho\bar{V}D/\eta$ , where  $\rho$  is fluid density,  $\Delta P$  required to reach given high  $Re$  scales like  $\Delta P \sim \Delta L/D^3$ . Therefore, if the channel’s proportions are preserved,  $\Delta P$  grows quadratically with  $1/D$  and when the channels are only a few tens of microns wide, achieving sufficiently high  $Re$  requires impractically high driving pressures.

In this Letter we present a microfluidic rectifier which can function at arbitrary low  $Re$  without any moving mechanical parts. Operation of the device is possible due to the nonlinear mechanical properties of the working fluid, which is a dilute aqueous solution of a flexible high molecular weight polymer. The nonlinear elastic properties of polymer solutions can lead to quite spectacular effects in macroscopic flows, including rod climbing (the Weissenberg effect) [3,4], dramatic growth of resistance in fast extensional flows [5], purely elastic

flow instabilities [6], and even elastic turbulence [7] at arbitrarily low  $Re$ . Recently it was shown that polymer solutions can be used as working liquids for functional nonlinear microfluidic devices [8]. The magnitude of the nonlinear elastic effects depends on the Weissenberg number [3],  $Wi = \lambda\nabla V$ , where  $\lambda$  is the relaxation time of the polymers and  $\nabla V$  is a characteristic rate of deformation in the flow.

A photograph of the microfluidic rectifier is shown in Fig. 1(a). The microchannel has a uniform depth  $h = 100 \mu\text{m}$  and is fabricated out of the silicone elastomer polydimethylsiloxane using soft lithography [9]. The functional nonlinear element is the middle channel, an enlarged image of a section of which is shown in Fig. 1(b). This channel is a chain of 43 identical segments, which are triangles, about  $230$  by  $330 \mu\text{m}$  in size, connected via bottleneck contractions of width  $d \approx 37 \mu\text{m}$ . The working fluid is a 0.01% by weight solution of a high molecular weight polyacrylamide ( $M_w = 1.8 \times 10^7$ , Polysciences). The Newtonian solvent was an aqueous solution of 13% sucrose, 1% NaCl, and 0.1% of the

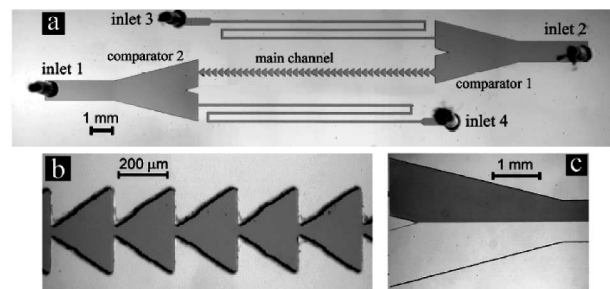


FIG. 1. (a) A photograph of the microfluidic rectifier. The channels were filled with ink for contrast. (b) A photograph of a fragment of the main channel. (c) A photograph of the comparator 1 with flow from left to right. The polymer solution flow is from the main channel (transparent liquid below) and flow of suspension of beads in the solvent is from the inlet 3 (dark liquid above).

surfactant Tween 20. The sucrose was added to bring the solution density to  $1.055 \text{ g/cm}^3$ , thus ensuring neutral buoyancy of suspended polystyrene beads used for flow visualization. NaCl was added to fix the ionic contents. The surfactant was added to facilitate filling of the microchannels, and it did not change rheological properties of the solution. The solvent viscosity,  $\eta_s$ , was  $1.37 \text{ cP}$  at room temperature, and the solution viscosity,  $\eta$ , was  $1.92 \text{ cP}$  at a shear rate of  $150 \text{ s}^{-1}$ . (The relation  $\eta/\eta_s \approx 1.4 < 2$  implies a dilute polymer solution.) The relaxation time,  $\lambda$ , was estimated as  $13 \text{ ms}$  from relaxation time measurements of the same polymer in a more viscous solvent [7], assuming that  $\lambda$  scales with  $\eta_s$  linearly [3].

The experimentally measured dependence of the volumetric flow rate,  $Q$ , through the rectifier on the pressure drop per segment,  $\Delta P$ , for the two flow directions is shown in Fig. 2. The flow was driven by hydrostatic pressure differences, which were generated using vertical rails with rulers and sliding stages. Working liquids were kept in  $30 \text{ cc}$  plastic syringes, which were positioned vertically and covered from above but not sealed. The syringes were attached to the sliding stages and connected to inlets and outlets by  $1.5 \text{ m}$  long plastic tubing with inner diameter  $0.76 \text{ mm}$ . The polymer solution forward flow was from inlet 1 to inlet 2 (the latter serving as an outlet in this case) [Fig. 1(a)], with the roles being reversed for the backward flow. For both cases the total pressure drop in the tubing together with comparator 1 and comparator 2 regions [Fig. 1(a)] was estimated to be below  $1\%$  of the pressure drop across the main channel.

The flow rates were measured using *in situ* compensation with the aid of the auxiliary flow channels [8]

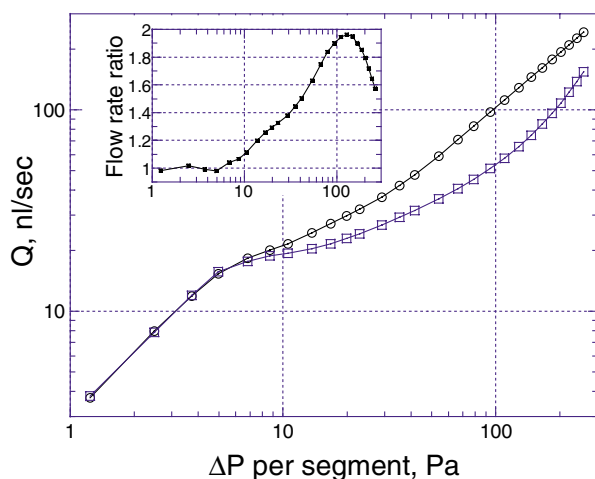


FIG. 2 (color online). Dependence of the volumetric flow rate,  $Q$ , of the polymer solution through the main channel on pressure drop per segment,  $\Delta P$ . The upper curve (circles) is for the forward flow and the lower curve (squares) is for the backward flow. Inset: Ratio of the flow rates,  $Q$ , between the flows forward and backward as a function of the pressure difference,  $\Delta P$ .

[Figs. 1(a) and 1(c)]. During the flow in the forward (backward) direction inlet 4 (3) was blocked and the Newtonian solvent with  $0.06\%$  (by volume) concentration of  $0.75 \text{ mm}$  polystyrene beads was fed from inlet 3 (4). The difference in liquid elevation between the syringes connected to the two inlets and the outlet was measured with a precision of about  $0.1 \text{ mm}$ , corresponding to  $1 \text{ Pa}$  in pressure. The flow of the polymer solution through the main channel and the flow of the solvent through an auxiliary channel merged in a comparator region, Fig. 1(c) (comparators 1 and 2 for the forward and backward flows, respectively). Because of low diffusivity of the beads and low flow rate in the comparator regions the boundary separating the two streams was always sharp and laminar. During the experiment the driving pressure ( $P_p$ ) for the polymer solution was gradually increased, and the pressure driving the flow of the solvent ( $P_s$ ) was tuned to maintain the separation line at the same position at the center of the comparator region, Fig. 1(c). After the dependence of  $P_s$  on  $P_p$  was found, the polymer solution was driven through the main channel at controlled  $Q$  using a syringe pump. Again,  $P_s$  was tuned to bring the separation line to the center, and a smooth curve connecting  $Q$  and  $P_s$  was obtained. Thus, we could calculate the dependence of  $Q$  on  $P_p$  (and on  $\Delta P = P_p/43$ ) for both flow directions with an estimated relative error of about  $0.5\%$ , which is mostly due to uncertainty in the adjustment of  $P_s$ .

Figure 2 shows that at low  $\Delta P$  and  $Q$  the dependence of  $Q$  on  $\Delta P$  is linear and identical for both flow directions. At  $Q \approx 17 \text{ nl/s}$  a transition occurs: the flow resistance starts to increase nonlinearly and the two curves diverge. The reason for the nonlinear growth of the flow resistance is that the polymer solution in the main channel is forced through a sequence of expansions and contractions. When a fluid element passes through a contraction it becomes extended along the flow direction, as do the polymer molecules inside it. If the rate of extension,  $\dot{\epsilon}$ , is sufficiently large compared to  $1/\lambda$ , the polymer molecules can unravel [10]. Their contribution to the flow resistance grows quickly and nonlinearly, so that the apparent viscosity of the polymer solution in a strong extensional flow may increase by a few orders of magnitude [5]. If we approximate the flow in front of a contraction as planar radial, the maximal rate of extension in the channel can be estimated as  $\dot{\epsilon} \approx Q/(2hd^2)$ , which gives  $\dot{\epsilon} \approx 62 \text{ s}^{-1}$  and  $Wi \equiv \lambda \dot{\epsilon} \approx 0.8$  at the transition point. That is consistent with  $Wi = 0.5$ , the expected value for the polymer unraveling transition [3,5,10,11]. For backward flow the resistance coefficient  $\Delta P/Q$  increases by up to a factor of  $6.3$  compared with the linear regime.

Nonlinear elastic flow transitions in channels with contractions are a well known phenomenon [3,4,12,13]. The increase in the resistance is comparable to that found in some macroscopic channels [14,15], and is smaller than a value reported recently for a specially designed

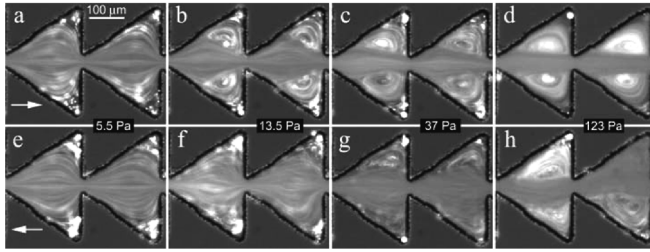


FIG. 3. Streakline patterns of flow of the polymer solution in the main channel at different pressure drops per segment,  $\Delta P$ . (a)–(d) The forward flow from left to right. (e)–(h) The backward flow from right to left.

microchannel [8]. The unusual property of the channel in Fig. 1, however, is that the flow resistance in the nonlinear regime is significantly different for the two flow directions. The inset to Fig. 2 shows that at  $\Delta P = 130$  Pa, the rate of flow from inlet 1 to inlet 2 is almost double that in the opposite direction. In a broad range of  $Q$ , from 43 to 90 nl/s, the required driving pressure for the backward flow is more than twice as high as for the forward flow. That implies a strong breaking of symmetry and a significant rectifying effect. The Reynolds number in the flow can be estimated as  $Q\rho/(h\eta)$ , giving  $Re = 0.3$  at  $Q = 60$  nl/s. Therefore, inertial effects are not of significance here.

A representative set of flow patterns observed in the main channel at different applied pressures is shown in Fig. 3. The flow was visualized by streaklines of  $1.1 \mu\text{m}$  yellow-green fluorescent beads. The beads were photographed using epifluorescent microscopy with a low numerical aperture  $10\times$  objective and a digital CCD camera. The exposure time was reduced and the illumination was increased as the flow rate became higher. At low applied pressure,  $\Delta P = 5.5$  Pa, Figs. 3(a) and 3(e), the streaklines for the both directions are indistinguishable, consistent with flow reversibility in the linear regime. When the pressure is raised to the nonlinear regime, however, the symmetry between the forward flow (Fig. 3, upper row) and the backward flow (Fig. 3, lower row) is broken.

The forward flow contains pairs of reentrant vortices, which appear in front of the contractions early in the nonlinear regime [Fig. 3(b)]. As  $\Delta P$  and  $Q$  are increased [Figs. 3(c) and 3(d)], the vortices grow in size, but they always remain symmetric and stationary. Appearance of reentrant vortices in front of contractions is quite common in flows of elastic polymer solutions in channels [3,4,8,14,15]. The situation in the backward flow is quite different. The reentrant vortices appear here at significantly higher driving pressures; they are smaller in sizes and continuously change their shapes, Figs. 3(f)–3(h). As shown in a time line recorded at  $\Delta P = 130$  Pa, Fig. 4, the backward flow pattern varies irregularly, with vortices in the corners that arise and vanish apparently randomly.

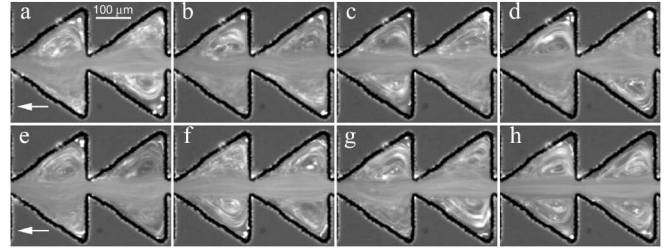


FIG. 4. A time series of streak line patterns for the backward flow of the polymer solution at  $\Delta P = 130$  Pa. The photographs were taken every 3 seconds, as the times progressed from (a) to (h).

These chaotic changes are reminiscent of the phenomenon of elastic turbulence [7].

An additional clue to the flow behavior can be obtained from streaklines at an even higher driving pressure,  $\Delta P = 250$  Pa, where the rectifying effect is reduced (Fig. 5). The pattern of flow in the forward direction, Fig. 5(a), looks similar to the pattern at  $\Delta P = 130$  Pa in Fig. 3(d). In contrast, the appearance of the backward flow, Figs. 5(b)–5(d), is significantly different than at  $\Delta P = 130$  Pa (Fig. 4); the fluctuations become small, the reentrant vortices are more stable, and the forward-backward symmetry in the flow is somewhat restored.

Analyzing the flow patterns in Figs. 3–5, we can conclude that the reasons for the nonlinear growth of the resistance in the two flow directions are essentially different. The forward flow remains stationary but becomes confined to a narrow tube around the central axis of the channel [Figs. 3(c) and 3(d)], and the cross sectional area of the tube does not change significantly along the channel. Therefore, the extensions and contractions are small compared with the shear, and the major contribution to the nonlinear resistance growth should come from the high shear stresses around the tube. In the backward flow confinement is much less significant [Figs. 3(g) and 3(h)], but fluid elements undergo a sequence of major random extensions and contractions as they move along the flow lines. That leads to significant growth of elastic stresses in the liquid [5,7], which probably provide the main contribution to the high resistance in the backward flow. We can conclude that the large elastic stresses produced by the chaotic backward flow lead to stronger growth of the flow

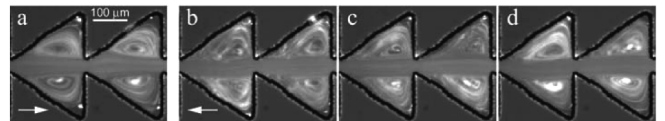


FIG. 5. (a) A typical streakline pattern of the polymer solution forward flow at  $\Delta P = 250$  Pa. (b)–(d) A time series of streakline patterns for the backward flow of the polymer solution at  $\Delta P = 250$  Pa. The photographs were taken every 5 seconds, as the times progressed from (b) to (d).

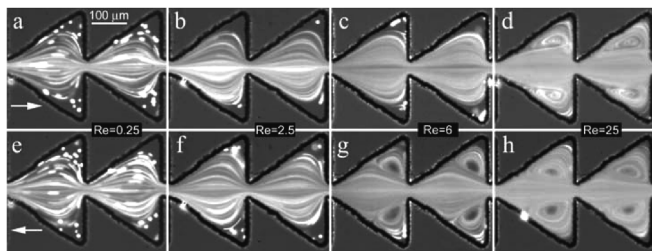


FIG. 6. Streakline patterns of flow of water in the main channel at different Reynolds numbers. (a)–(d) The flow is from left to right (forward). (e)–(h) The flow is from right to left (backward).

resistance than the high shear stresses associated with the confinement in the forward flow. That appears to be the physical basis of the anisotropic resistance and rectifying effect (Fig. 2).

It is instructive to compare the flow of the polymer solution with the Newtonian flow of water through the same channel at low to moderate  $Re$  (Fig. 6). The total pressure drop across the channel for  $Re = 25$  was about 30 kPa; higher Reynolds numbers could not be reached in the present apparatus. The flow remains linear and reversible up to  $Re \approx 3$  [Figs. 6(a), 6(b) and 6(e), 6(f)]. At higher Reynolds numbers the inertial nonlinearity sets in and the patterns of the forward and backward flows become different [Figs. 6(c), 6(d) and 6(g), 6(h)]. There is obvious similarity between the following pairs of patterns: Fig. 6(g)/Fig. 3(b), Fig. 6(h)/Fig. 3(c), and Fig. 6(d)/Fig. 3(g), respectively. Those are, however, flows in opposite directions. Indeed, nonlinearity in the flow in Fig. 6 arises at rather high  $Re$  and it is of an inertial nature. Therefore, the vortices in Figs. 6(g) and 6(h) appear behind the contractions [rather than in front of them as in Figs. 3(b)–3(d)] and they are due to energetic inertial jets formed at the contractions. Thus, one can say that elasticity works in a manner opposite to inertia.

In summary, we have designed and tested a microfluidic rectifier. This microscopic channel geometry shows up to a twofold difference in resistance for flows in opposite directions. The device operates with an aque-

ous solution to which only 0.01% of a high molecular weight polymer was added (increasing the viscosity by only 40%). Since it can operate at arbitrarily small Reynolds numbers, it can be scaled down, and we indeed have observed similar flow effects in a 4 times smaller device at comparable driving pressures. We believe that this rectifier, which acts similarly to a diode or a dynamic valve, can find applications for micropumps and complex integrated microfluidic circuits and control devices.

\*Current address: Department of Physics, UC San Diego, 9500 Gilman Drive, La Jolla, CA 92093, USA.

†To whom correspondence should be addressed.

Electronic address: quake@caltech.edu

- [1] N. Tesla, Valvular Conduit, U.S. Patent No. 1 329 559.
- [2] L. D. Landau and E. M. Lifshitz, *Fluid Mechanics* (Pergamon Press, New York, 1987).
- [3] R. B. Bird, Ch. Curtiss, R. C. Armstrong, and O. Hassager, *Dynamics of Polymeric Liquids* (Wiley, New York, 1987), Vols. 1,2.
- [4] D. V. Boger and K. Walters, *Rheological Phenomena in Focus* (Elsevier Science Publishers, Amsterdam, 1993).
- [5] V. Tirtaatmadja and T. Sridhar, *J. Rheol.* **37**, 1081 (1993).
- [6] S. J. Muller, R. G. Larson, and E. S. G. Shaqfeh, *Rheol. Acta* **28**, 499 (1989).
- [7] A. Groisman and V. Steinberg, *Nature (London)* **405**, 53 (2000).
- [8] A. Groisman, M. Enzelberger, and S. R. Quake, *Science* **300**, 955 (2003).
- [9] X. Xia and G. M. Whitesides, *Angew. Chem., Int. Ed. Engl.* **37**, 551 (1998).
- [10] P. G. DeGennes, *J. Chem. Phys.* **60**, 5030 (1974).
- [11] Another important parameter which needs to be sufficiently large for polymer coil unraveling is logarithm of the total strain in the flow region where  $Wi > 0.5$ . Here it is of order unity at the transition point.
- [12] C. Petrie and M. Denn, *AIChE J.* **22**, 209 (1976).
- [13] R. G. Larson, *Rheol. Acta* **31**, 213 (1992).
- [14] U. Cartalos and J. M. Piau, *J. Non-Newtonian Fluid Mech.* **45**, 231 (1992).
- [15] J. P. Rothstein and G. H. McKinley, *J. Non-Newtonian Fluid Mech.* **98**, 33 (2001).